

Sensor and Simulation Notes

Note 55

May 1968

Interaction Between a Cylindrical Test Body and a
Parallel Plate Simulator

R. W. Latham

Northrop Corporate Laboratories
Pasadena, California 91101

Abstract

The charge distribution on a cylindrical test body whose axis is parallel to the plates of a two-plate transmission line simulator, and the fields near the test body, are computed. These charges and fields are compared with the desired distributions, i.e. those that occur when the cylinder is of negligible size compared to the plate spacing. Some interesting mathematically related problems are also discussed.

CLEARED
FOR PUBLIC RELEASE

PL/PA 10/27/94

PL 94-0925

NOTE 55

INTERACTION BETWEEN A CYLINDRICAL TEST
BODY AND A PARALLEL PLATE SIMULATOR

by

R.W. Latham
Northrop Corporate Laboratories

May 1968

ABSTRACT

The charge distribution on a cylindrical test body whose axis is parallel to the plates of a two-plate transmission line simulator, and the fields near the test body, are computed. These charges and fields are compared with the desired distributions, i. e. those that occur when the cylinder is of negligible size compared to the plate spacing. Some interesting mathematically related problems are also discussed.

Acknowledgment

The author wishes to thank Dr. Kelvin Lee and Capt. Carl Baum for their interest in this problem, Mr. Dick Sassman for the numerical calculations, and Mrs. Georgene Peralta for typing the manuscript.

I. Introduction

The effect of the low frequency portion of the spectrum of the electromagnetic pulse from a nuclear burst on buried structures can be simulated by a buried parallel plate transmission line¹. If this simulation technique is used a question arises concerning the accuracy with which the simulator fields represent the desired fields in the vicinity of the test body. The desired fields are those occurring when the interaction between the test body and the parallel plate structure can be neglected. This interaction can be neglected when the test body is of negligible size compared to the plate spacing, so the question mentioned above may be stated more precisely: how large can a test body be compared to the plate spacing, and still have the fields in its vicinity within a certain percentage of those fields induced when the plates creating the external field are infinitely far apart? Although one can always be sure of the accuracy of the simulation by making the plate structure very large, this question should be answered because the engineering problems increase greatly with the size of the buried line. In this note an accurate solution to a somewhat idealized version of the problem is presented. The data presented here will be useful in determining the necessary ratio of plate spacing to buried structure size once the allowable error of the field values in the neighborhood of the structure is decided upon.

The model problem chosen for solution here is that of an infinite circular cylinder centered between two infinite parallel plates. The plates, far from the cylinder, are assumed to be sustaining a uniform TEM wave propagating parallel to the axis of the cylinder. The geometry of this model, and the excitation method, resemble the situation of a two plate line exciting a buried cylindrical structure with a metallic shield (see figure 1) since the waves propagating in this realistic case are also almost TEM waves. The TEM nature of the waves simplifies the problem requiring mathematical solution by reducing it to a two-dimensional electrostatic problem. The geometry of this electrostatic problem is shown in figure 2. Between the two plates of figure 2, and at a large distance from the cylinder, an electric field perpendicular to the plates and of magnitude E_0 is assumed to exist. We wish to calculate the fields in the neighborhood of the cylinder. This will be

done by first calculating the surface charge density induced on the cylinder. This charge density is proportional to the normal electric field at the surface of the cylinder. Furthermore it is proportional to the tangential magnetic field and the longitudinal surface current density in the TEM transmission line situation. But the most important fact about this surface charge density is that once it is known the fields anywhere between the plates can be computed by simple summation techniques as shown in the next section.

The next section deals with the mathematical solution to the electrostatic problem described above. Since the method of solution is not too common, and may be of interest in itself, Section III presents a brief discussion of a few other geometrical configurations whose electrostatic properties can be determined by similar mathematical techniques. In Section IV accurate numerical data on the primary problem is presented, along with a few words of explanation. Some of the algebraic details of the problem are relegated to the appendices.

II. A Cylinder Between Two Plates

The real problem to be analysed is shown schematically in figure 1, but as mentioned in the introduction, if the parallel plates of figure 1 are assumed to be sustaining a TEM wave, the transverse electric field at any horizontal cross-section of the simulator is well represented by the two-dimensional electrostatic field within the two infinite plates of figure 2. The fields of the model problem of figure 2 will be computed by a method which is in one way an extension, and in another way a specialization, of a method originally due to Lord Rayleigh². Rayleigh computed the average conductivity of a cubic lattice of perfectly conducting spheres embedded in an imperfect conductor, taking into account only dipole interactions. In the present problem, by replacing the plates with an infinite set of image cylinders, it is seen that it is necessary to compute the surface charge density on an infinite row of cylinders taking into account all multipole interactions.

The solution of the two-dimensional problem begins by representing the surface charge distribution on the primary cylinder of figure 2 by means of a Fourier series in the angular variable θ_o .

$$\sigma_o(\theta_o) = \sum_{n=0}^{\infty} s_n \cos n\theta_o \quad (1)$$

It should be noted here that, contrary to the usual notation, the angular variable θ_o is chosen to be measured from the y-axis for reasons of simplicity in presentation.

In order to make the discussion as concise as possible we now state without demonstration three facts which would become evident after a more lengthy examination of the problem:

- (1) The field between the plates can be considered to be the linear superposition of the external field and the field due to the charges on the cylinder and all its images. The field due to the charges on the plates is entirely accounted for by the fictitious charges on the set of image cylinders.

- (2) The charge densities on all the even numbered image cylinders are the same as that given by (1) while the densities on the odd numbered cylinders are:

$$\sigma_{2n+1}(\theta_{2n+1}) = -\sigma_o(\pi - \theta_{2n+1}) \quad (2)$$

- (3) The potential outside the cylinder due to the net charges on the set of image cylinders, i.e. the potential due to a set of line charges of alternating sign, may be accounted for by solving with the aid of a conformal transformation the simple electrostatic problem of a line charge between two plates. This procedure is advisable because it avoids the possibility of summing in an improper manner the conditionally convergent series resulting from adding the individual contributions of the image line charges.

Using these facts, after some algebraic manipulations it can be shown that the potential between the plates and outside the cylinder is

$$\begin{aligned} \phi_e(x,y) = \phi_o(x,y) + \frac{s_o a}{2\epsilon_o} \ln \left[\frac{\cosh(\pi x/D) + \cos \pi(y + y_o)/D}{\cosh(\pi x/D) - \cos \pi(y - y_o)/D} \right] \\ + \sum_{n=1}^{\infty} \sum_{m=-\infty}^{\infty} \frac{(-1)^{n+m} s_n a}{2n\epsilon_o} \left(\frac{a}{r_m} \right)^n \cos(n\theta_m) \end{aligned} \quad (3)$$

where y_o , r_m , and θ_m are as shown in figure 2, and $\phi_o(x,y)$ is the potential of the external field. A little more detail concerning the derivation of equation (3) is given in Appendix A.

Within the cylinder the potential due to the charge on the primary cylinder itself has a slightly different form. This different form is such that, within the cylinder and on the y axis, the total potential may be written as:

$$\begin{aligned} \phi_i(0,y) = \phi_o(0,y) + \frac{s_o a}{2\epsilon_o} \ln \left[\frac{1 + \cos \pi(y + y_o)/D}{1 - \cos \pi(y - y_o)/D} \right] \left[\frac{y - y_o}{a} \right]^2 \\ + \sum_{n=1}^{\infty} \sum_{m=-\infty}^{\infty} \frac{(-1)^{n+m} s_n a}{2n\epsilon_o} \left(\frac{a}{r_m} \right)^n \cos(n\theta_m) + \sum_{n=1}^{\infty} \frac{s_n a}{2n\epsilon_o} \left(\frac{y}{a} \right)^n \end{aligned} \quad (4)$$

where the prime on the summation indicates the omission of the $m = 0$ term. Of course in equation (4) r_m and θ_m are simple functions of y , y_0 , and m , but the representation given is more concise.

Within the cylinder, which is assumed to be perfectly conducting, the total potential must be independent of position. This may be assured by equating $\phi_i(0,0)$ to some number, V , and by setting all the y derivatives of $\phi_i(0,y)$ equal to zero at the origin. That this procedure will lead to a potential which is constant everywhere within the cylinder follows from the nature of Laplace's equation. Another procedure leading to the same set of conditions on the constants s_n would be to expand equation (3) in a Fourier cosine series in θ_0 and to equate all the resulting Fourier constants to zero except the first. Either of these methods leads to the following set of equations.

$$\begin{aligned} \frac{V - \phi_0(0,0)}{a} &= x_0 \ln\left(\frac{2D}{\pi a}\right) + \sum_{n=1}^{\infty} \frac{x_n \left(\frac{a}{D}\right)^n}{n} \left[\sum_{m=-\infty}^{\infty} \frac{1}{(2m)^n} - \sum_{m=-\infty}^{\infty} \frac{1}{(2m-1+2y_0/D)^n} \right], \\ - a^{\ell-1} \phi_0^{\ell}(0,0) &= x_{\ell} \tag{5} \\ + \sum_{n=0}^{\infty} \frac{x_n (n+\ell-1)!}{n! (\ell-1)!} \left(\frac{-a}{D}\right)^{n+1} &\left[\sum_{m=-\infty}^{\infty} \frac{(-1)^n}{(2m)^{n+\ell}} - \sum_{m=-\infty}^{\infty} \frac{1}{(2m-1+2y_0/D)^{n+\ell}} \right] \quad \ell > 0 \end{aligned}$$

where

$$x_{\ell} = (1 + \delta_{0\ell}) s_{\ell} / 2\epsilon_0$$

In general these equations must be solved to determine the constants x_{ℓ} . The field between the plates may then be calculated from the gradient of equation (3). For the remainder of this section the equations will be specialized to the case where y_0 is zero. This simplifies equations (5) considerably by decoupling the even ordered coefficients from the odd ordered

coefficients. Two particular cases will be studied in more detail.

Case 1:

If

$$\phi_0(x,y) = -E_0 y$$

all the even coefficients are zero while the equations determining the odd coefficients may be written as follows:

$$C_{2n-1} - 2 \sum_{m=1}^{\infty} \left(\frac{a}{D}\right)^{2(n+m-1)} \binom{2n+2m-1}{2n-2} \zeta(2n+2m) C_{2m-1} = \delta_{n,1} \quad , \quad n > 0 \quad (6)$$

where $\zeta(z)$ is the Riemann Zeta function³ and the dimensionless constants C_{2n-1} are equal to x_{2n-1}/E_0 . This choice of normalization leads to the following simple solution when the effect of the plates can be neglected:

$$C_{2n-1} = \delta_{n,1} \quad .$$

The charge density in this case of very large plate spacing is:

$$\sigma_L(\theta_0) = 2\epsilon_0 E_0 \cos \theta_0 \quad . \quad (7)$$

In addition to this asymptotic form the opposite case of small plate spacing compared to cylinder diameter may be studied with the aid of the solution to the elementary electrostatic problem of two coupled cylinders⁴. This study leads to the following approximate form:

$$\sigma_S(\theta_0) = 2\epsilon_0 E_0 \frac{D(1 + D/d)}{4\sqrt{(d+\Delta)\Delta} \cosh^{-1}(D/d)} \cdot \frac{1}{\cos \theta_0 + d/2\Delta(1 - \cos \theta_0)} \quad , \quad \theta < \pi/2 \quad (8)$$

where

$$\Delta = (D - d)/2 \quad .$$

For the largest cylinder that was studied, and for θ_0 equal to zero, equation (8) is in error by less than one part in a thousand.

Another quantity of interest in the case now under study is the incremental transmission line admittance of the parallel plate structure due to the presence of the cylinder. The value of this quantity is given by the following expression:

$$\frac{\Delta Y_L}{Y_0} = \frac{\pi \left(\frac{a}{D}\right)^2}{2} C_1 \quad (9)$$

This simple relation may be arrived at by computing the total extra charge on the top plate and relating this extra charge to the change in transmission line capacity per unit length. The extra charge can be computed by integrating with respect to x the y -derivative of equation (3) for y equal to $D/2$, omitting that portion of the y -derivative due to the external field. Although equation (9) is rigorously true only for plates of infinite width, it will still be a good approximation to the change in transmission line admittance of a two plate line of finite width due to the presence of a cylinder as long as the plate width is greater than the plate spacing.

The charge density on the cylinder, in the case under study, is

$$\frac{\sigma(\theta)}{2\epsilon_0 E_0} = \sum_{n=1}^{\infty} C_{2n-1} \cos(2n-1)\theta$$

The special forms that the derivatives of equation (3) take for the case now under study will be omitted here since those expressions are only of interest for efficient computer programming.

Case 2:

If

$$\phi_o(x,y) = 0$$

and

$$V \neq 0$$

equations (5) reduce to

$$C_o \ln \left(\frac{2D}{\pi a} \right) - \sum_{m=1}^{\infty} \left(\frac{a}{D} \right)^{2m} \frac{(1-2^{1-2m})}{m} \zeta(2m) C_{2m} = 1 \quad (10)$$

$$C_{2n} - 2 \sum_{m=0}^{\infty} \left(\frac{a}{D} \right)^{2(n+m)} \binom{2n+2m-1}{2n} (1-2^{1-2(n+m)}) \zeta(2n+2m) C_{2m} = 0, \quad n > 0$$

where

$$C_{2n} = x_{2n} a/V$$

Asymptotic forms similar to those derived in the previous case could also be derived here. But since the present case is not directly connected to the primary problem, and is included only as a matter of interest, we restrict ourselves to writing the charge density

$$\frac{\sigma(\theta)a}{\epsilon_o V} = \sum_{n=0}^{\infty} C_{2n} (1 + \delta_{on}) \cos 2n\theta, \quad ,$$

and the transmission line admittance of this structure

$$\frac{Y_L}{Y_o} = 2\pi C_o \quad (11)$$

III. Mathematically Related Problems

The method of solution used in Section II is very old. As mentioned before, to the author's knowledge Rayleigh was the first to use similar techniques to solve a problem involving an infinite number of bodies. But the essence of the method can be found already in the works of Maxwell⁵ who used it to determine the capacity between two spheres of unequal size. However, in spite of the age of the method and its rather special nature, there are still several problems to which it could profitably be applied. Therefore it seems worthwhile to try to pick out the essential characteristics of the procedure used in the previous section and to point out some electromagnetic problems amenable to similar solutions and for which no precise calculations have yet been made.

One feature of the problem that made the solution of the previous section feasible was the simple connections that both the internal and external potentials have with the surface charge density on a cylinder. These connections are given explicitly by equations (A-2) and (A-3). The reason why these relations must be simple is that the method involves writing an explicit representation of the n^{th} derivative of both the internal and external potentials with respect to some Cartesian coordinate variable. Besides the cylinder, the sphere is the only other geometrical shape for which such representations may be easily written down.

Another essential feature of the problem of the previous section is that it is reducible to one involving only cylinders. This reduction is already accomplished if there are actually only cylinders present but it is also possible if there are infinite planes present but situated in such a way that their effect may be accounted for by one or more image cylinders.

Most of the remainder of this section consists of two brief discussions. The first discussion is of the problem in which a sphere replaces the cylinder between the two plates of the last section. The second discussion is of a problem analogous to case 2 of the last section, the cylinder being now completely enclosed by four conducting plates to form a type of coaxial transmission line. A few other configurations where the present techniques may be applied are only mentioned.

Example 1:

A coordinate system and system of notation that may be used for mathematically determining the electrostatic capacity between a sphere and two parallel plates equidistant from it are shown in the schematic diagram for this problem, figure 3A.

Using that system of notation and following a procedure exactly analogous to that used in Section II and Appendix A, it is possible to write the charge density on the sphere as

$$\sigma(\theta) = \sum_{n=0}^{\infty} s_{2n} P_{2n}(\cos \theta) \quad ,$$

where P_{2n} is a Legendre polynomial of order $2n$ and s_{2n} is an unknown coefficient, the potential at the center of the sphere must be

$$V = \frac{s_0 a}{\epsilon_0} + \sum_{n=0}^{\infty} \frac{s_{2n} a}{(4n+1)\epsilon_0} \sum_{m=-\infty}^{\infty} (-)^m \left| \frac{a}{mD} \right|^{2n+1} \quad ,$$

while setting the $2\ell^{\text{th}}$ z -derivative of the potential equal to zero at the center of the sphere gives

$$0 = \frac{s_{2\ell}}{4\ell+1} \frac{a}{\epsilon_0} \frac{(2\ell)!}{a^{2\ell}} + \sum_{n=0}^{\infty} \frac{s_{2n} a}{(4n+1)\epsilon_0} \sum_{m=-\infty}^{\infty} (-)^m \frac{(2n+2\ell)!}{(2n)!} \frac{a^{2n+1}}{|mD|^{2n+2\ell+1}} \quad .$$

It may be noted here that in this three dimensional case no delicate convergence problems such as those arising in the second section occur.

Now introducing a new set of unknown coefficients in the above equations by the definitions

$$x_{2\ell} = \frac{s_{2\ell} a}{(4\ell+1)\epsilon_0 V}$$

it easily follows that the capacity between the sphere and the two plates, C , normalized to the capacity of the sphere in free space, $4\pi\epsilon_0 a$, is given by the first unknown x_0 . In other words

$$\frac{C}{4\pi\epsilon_0 a} = x_0$$

where

$$\sum_{m=0}^{\infty} M_{nm} x_{2m} = \delta_{n,0}$$

and

$$M_{nm} = \delta_{n,m} - 2 \frac{(2n+2m)!}{(2n)!(2m)!} (1-2^{-(2n+2m)}) \zeta(2n+2m+1) \left(\frac{a}{D}\right)^{2n+2m+1}$$

Example 2:

The coordinate systems used to compute the input admittance of a transmission line consisting of a circular cylinder at the center of a rectangular cylinder may be chosen to be the same as that used in Section II. The exact geometry of this line, and the extra notation now necessary, are shown in figure 3B.

In the present case the effect of the walls of the enclosing rectangular cylinder on the potential distribution within the line can be accounted for by a two dimensional lattice of image cylinders. For this reason it follows that the potential at the origin due to the zeroth Fourier component of charge on the cylinder may be written, using the representation of the potential of a vertical row of line charges implicit in (3), as

$$\frac{V_0}{C_0} = \frac{a}{\epsilon_0} \ln \frac{2D}{\pi a} - \frac{2a}{\epsilon_0} \sum_{n=1}^{\infty} (-)^n \ln \tanh \left(\frac{\pi}{2} \frac{D}{D} \frac{x}{y} n \right) \quad (12)$$

Using the methods of Section II to calculate this same quantity but summing first over a horizontal row of line charges one clearly would obtain

$$\frac{V_o}{C_o} = \frac{a}{\epsilon_o} \ln \frac{2D_x}{\pi a} - \frac{2a}{\epsilon_o} \sum_{n=1}^{\infty} (-)^n \ln \tanh \left(\frac{\pi}{2} \frac{D_y}{D_x} n \right) \quad (13)$$

This equation seemingly is different from equation (12) but writing the first term of (12) as

$$\frac{a}{\epsilon_o} \ln \frac{2D_y}{\pi a} = \frac{a}{\epsilon_o} \ln \frac{2D_x}{\pi a} - \frac{a}{\epsilon_o} \ln \frac{D_x}{D_y}$$

and employing the relation proven in Appendix B equations (12) and (13) are seen to be identical. This is the only difficult point in the present problem. The procedure is now similar to that of case 2 of Section II, the input admittance of the line will again be determined by equation (11) and the unknowns will be determined by equations like (10). The only difference is that the matrix elements of the equations analogous to (10) will now involve, in addition to the functions they previously depended upon, the $(2n+2m-1)^{\text{th}}$ derivative of a function defined by

$$f(y) = \sum_{m=-\infty}^{\infty} (-)^m \operatorname{csch} \left[(y - mD_y) / D_x \right]$$

Some of the other geometrical configurations to which the present methods could be applied are: two cylinders between the two plates of Section II, a cylinder within the quadrant formed by two planes intersecting at right angles, and a sphere within a rectangular parallelepiped.

IV. Numerical Results

The quantitative data displayed in the following tables and graphs is limited to the two special cases of Section II. The sets of equations (6) and (10) were solved numerically, keeping only ten equations and ten unknowns in each case. They were then resolved, keeping twenty equations and twenty unknowns. The difference in the charge densities computed by means of these two solutions was so small, even for the largest cylinders studied, that the numerical data for the twenty by twenty solution can be considered to be accurate to five digits. Although for engineering and qualitative purposes the graphical data given in figures 4 through 9 might be sufficient, for the sake of completeness, and for possible future needs, some of the data is given in a more definite and accurate form in tables I through V. The numbers in the tables are accurately rounded to the number of digits given.

Table I gives the surface charge density at three points on a cylinder centered between two infinite plates sustaining a uniform electric field of value E_0 at a large distance from the cylinder. These values of surface charge are normalized to the values they would attain if the interaction between the cylinder and the plates were negligible. The values are tabulated as a function of cylinder size. It is of interest to note that the asymptotic form given in equation (8) predicts, for $\theta = 0$ and $d/D = .96$, that $\sigma(\theta)/2\epsilon_0 E_0$ would be 12.671 while the tabulated value is 12.673.

Tables II and III contain the Fourier constants computed from equations (6) and (10) respectively. These constants may be used to compute accurate values of charge for positions other than those given in table I. These tables may also be useful in connection with equations (9) and (11).

Table IV gives accurate normalized values of the electric field at the plane midway between the plates for the problem defined in Section II as case 1. Table V gives the same kind of information for positions along the top plate.

Figure 4 shows the charge density on various sizes of cylinder for case 1 while figure 5 contains the same type of information for case 2.

Figure 6A shows the data of table I in graphical form while figure 6B contains similar data for case 2.

Figures 7 and 8 contain the same type of information as tables IV and V but for a greater number of cylinder sizes.

Figures 9A and 9B are plots of equations (6) and (11) respectively.

TABLE I

$$\sigma(\theta)/2\epsilon_0 E_0$$

$d/D \backslash \theta$	0°	30°	60°
.00	1.000	.866	.500
.04	1.001	.867	.501
.08	1.005	.871	.503
.12	1.012	.876	.506
.16	1.022	.885	.510
.20	1.035	.895	.516
.24	1.051	.909	.523
.28	1.072	.926	.532
.32	1.097	.946	.541
.36	1.127	.969	.552
.40	1.164	.997	.564
.44	1.209	1.029	.577
.48	1.263	1.066	.592
.52	1.329	1.110	.607
.56	1.411	1.161	.624
.60	1.511	1.221	.641
.64	1.637	1.292	.660
.68	1.799	1.376	.680
.72	2.011	1.477	.702
.76	2.298	1.599	.724
.80	2.705	1.751	.749
.84	3.321	1.942	.774
.88	4.354	2.192	.802
.92	6.430	2.528	.831
.96	12.673	3.005	.863

TABLE II
FOURIER COEFFICIENTS OF CYLINDER SURFACE CHARGE (Case 1)

COEFF. d/D	C_1	C_3	C_5	C_7	C_9	C_{11}
.00	1.000					
.04	1.001					
.08	1.005					
.12	1.012					
.16	1.022					
.20	1.034	.001				
.24	1.050	.001				
.28	1.069	.003				
.32	1.092	.005				
.36	1.119	.008				
.40	1.152	.012	.001			
.44	1.190	.018	.001			
.48	1.234	.027	.002			
.52	1.287	.038	.004			
.56	1.349	.054	.007	.001		
.60	1.423	.076	.011	.001		
.64	1.512	.105	.017	.003		
.68	1.621	.145	.027	.005	.001	
.72	1.756	.201	.043	.008	.001	
.76	1.930	.280	.069	.015	.003	.001
.80	2.160	.395	.112	.029	.007	.001

TABLE III
FOURIER COEFFICIENTS OF CYLINDER SURFACE CHARGE (Case 2)

COEFF. d/D	C_0	C_2	C_4	C_6	C_8	C_{10}
.00	.000					
.04	.289					
.08	.361	.001				
.12	.423	.003				
.16	.482	.005				
.20	.540	.009				
.24	.599	.014				
.28	.661	.021				
.32	.725	.031	.001			
.36	.792	.042	.002			
.40	.865	.057	.003			
.44	.944	.076	.004			
.48	1.030	.099	.007			
.52	1.125	.128	.011	.001		
.56	1.230	.164	.016	.001		
.60	1.350	.210	.024	.003		
.64	1.487	.267	.035	.005	.001	
.68	1.646	.340	.053	.008	.001	
.72	1.837	.435	.079	.014	.002	
.76	2.070	.562	.119	.025	.005	.001
.80	2.366	.738	.184	.045	.011	.003

TABLE IV
NORMALIZED E-FIELD MIDWAY BETWEEN PLATES

$x/a \backslash d/D$.2	.4	.6	.8
1.0	.000	.000	.000	.000
1.2	.315	.341	.377	.415
1.4	.505	.546	.599	.653
1.6	.629	.677	.736	.792
1.8	.713	.765	.824	.875
2.0	.773	.826	.881	.924
2.2	.817	.870	.920	.953
2.4	.851	.902	.945	.971
2.6	.877	.925	.962	.982
2.8	.897	.943	.974	.989
3.0	.914	.956	.982	.993
3.2	.927	.966	.988	.995
3.4	.938	.974	.991	.997
3.6	.947	.980	.994	.998
3.8	.955	.984	.996	.998
4.0	.961	.988	.997	.999

TABLE V
NORMALIZED E-FIELD AT TOP PLATE

$x/D \backslash d/D$.2	.4	.6	.8
0.0	1.102	1.455	2.281	4.717
0.2	1.070	1.313	1.871	3.325
0.4	1.028	1.126	1.343	1.827
0.6	1.009	1.040	1.108	1.249
0.8	1.003	1.012	1.032	1.072
1.0	1.001	1.003	1.009	1.021
1.2	1.000	1.001	1.003	1.006
1.4	1.000	1.000	1.001	1.002
1.6	1.000	1.000	1.000	1.001
1.8	1.000	1.000	1.000	1.001
2.0	1.000	1.000	1.000	1.000

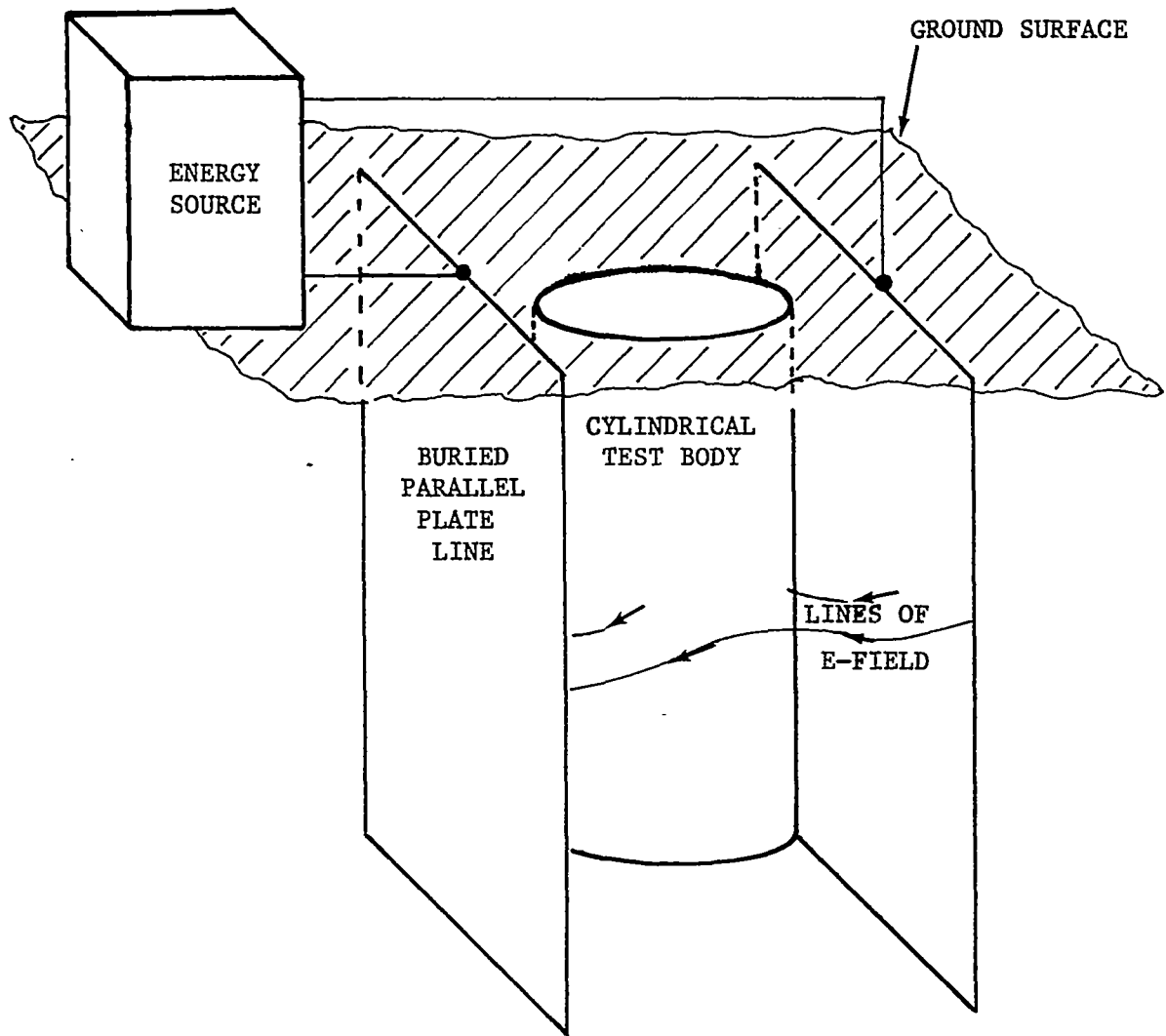


FIGURE 1: A CYLINDRICAL TEST BODY IN A PARALLEL PLATE TRANSMISSION LINE SIMULATOR

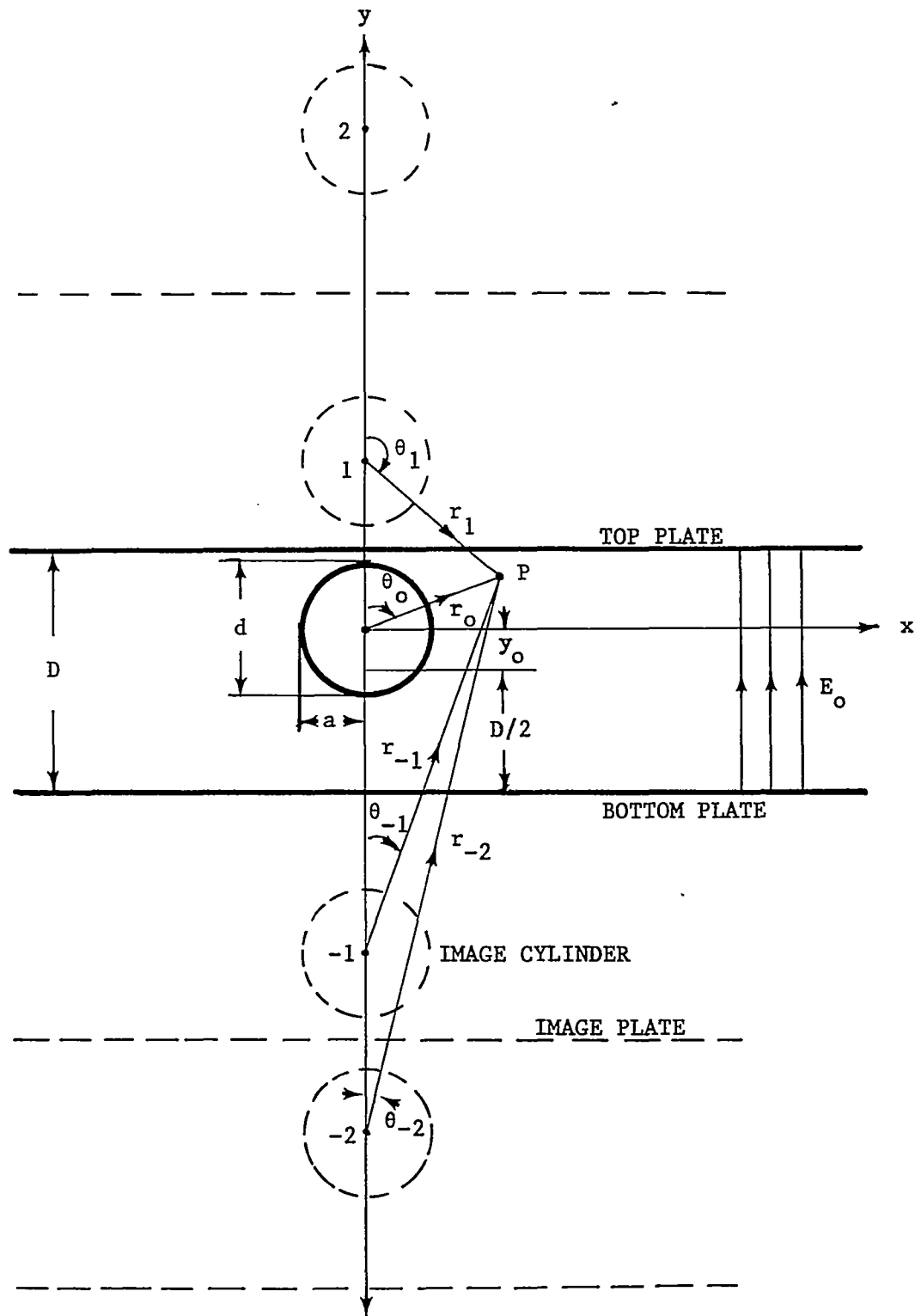
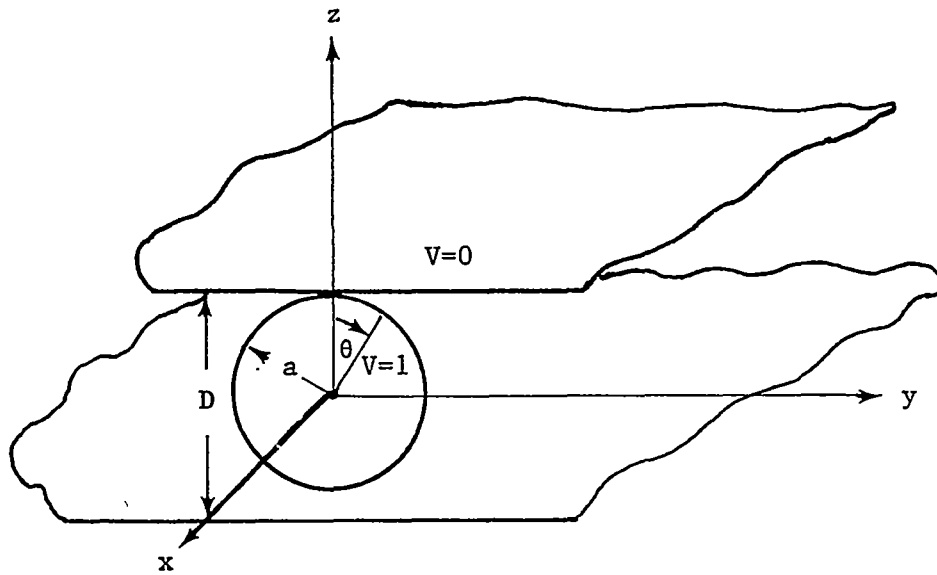
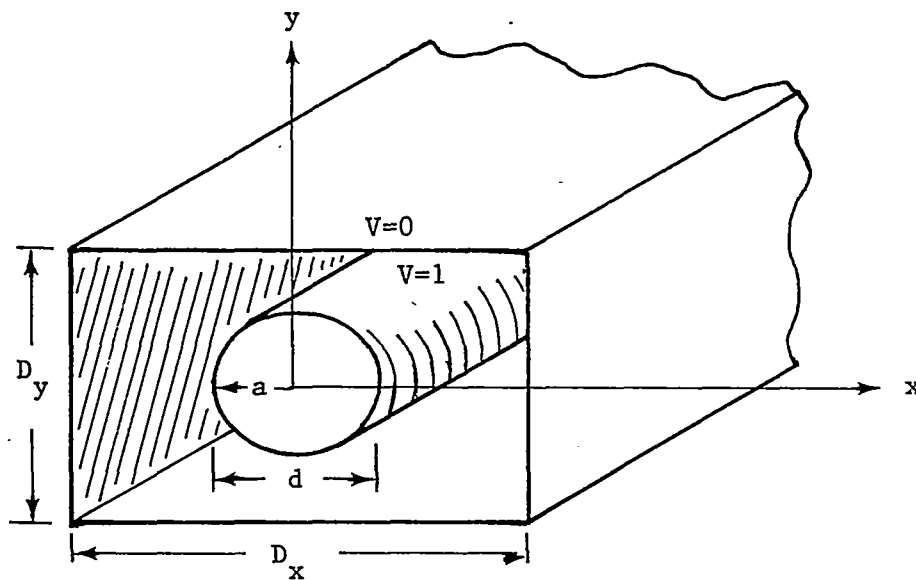


FIGURE 2: TWO-DIMENSIONAL ELECTROSTATIC CONFIGURATION WHOSE FIELDS ARE COMPUTED IN SECTION II



A: A SPHERE BETWEEN PARALLEL PLATES



B: A CIRCULAR CYLINDER WITHIN A RECTANGULAR CYLINDER

FIGURE 3: MATHEMATICALLY RELATED
ELECTROSTATIC PROBLEMS

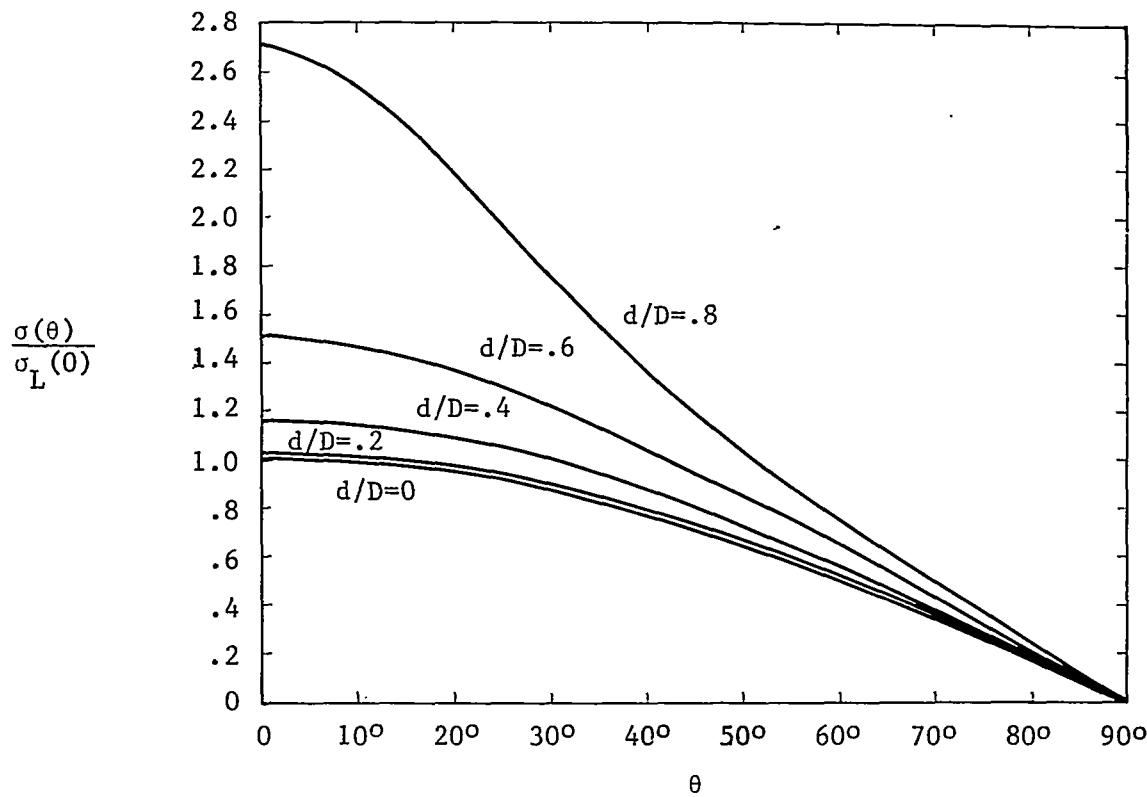


FIGURE 4A: CHARGE DENSITY ON SMALL CYLINDERS

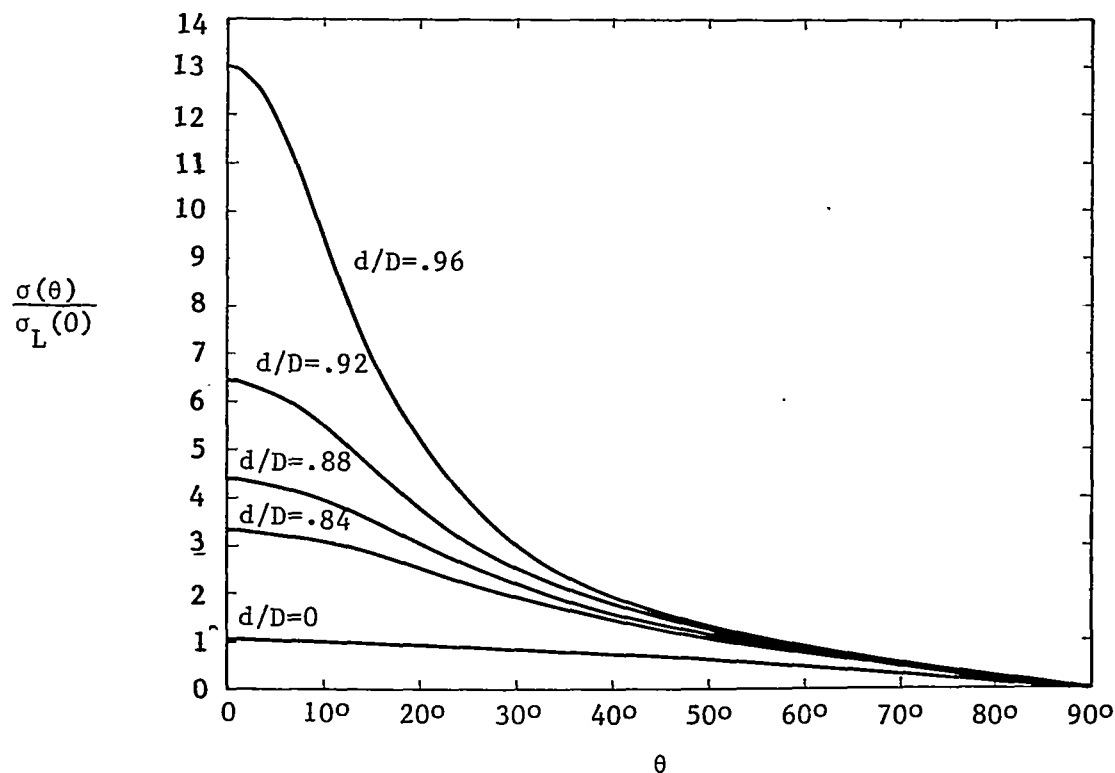


FIGURE 4B: CHARGE DENSITY ON LARGE CYLINDERS

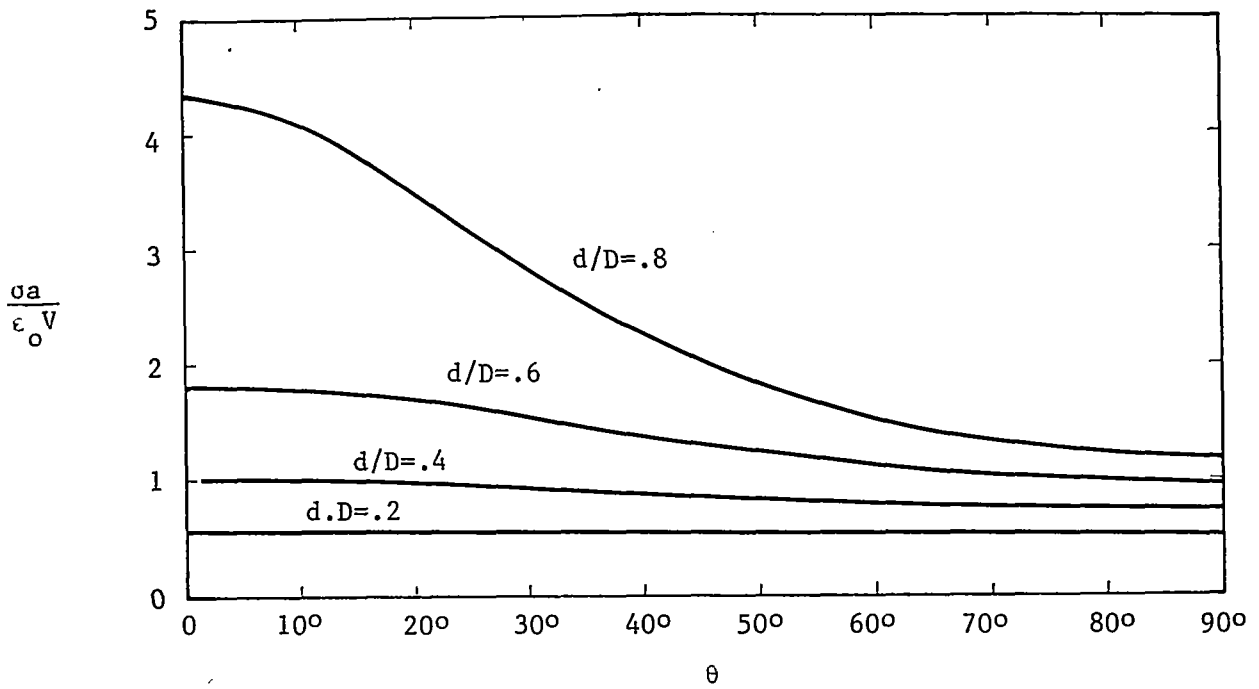


FIGURE 5A: CHARGE DENSITY ON SMALL CYLINDERS, LINE DRIVEN BETWEEN CYLINDER AND PLATES

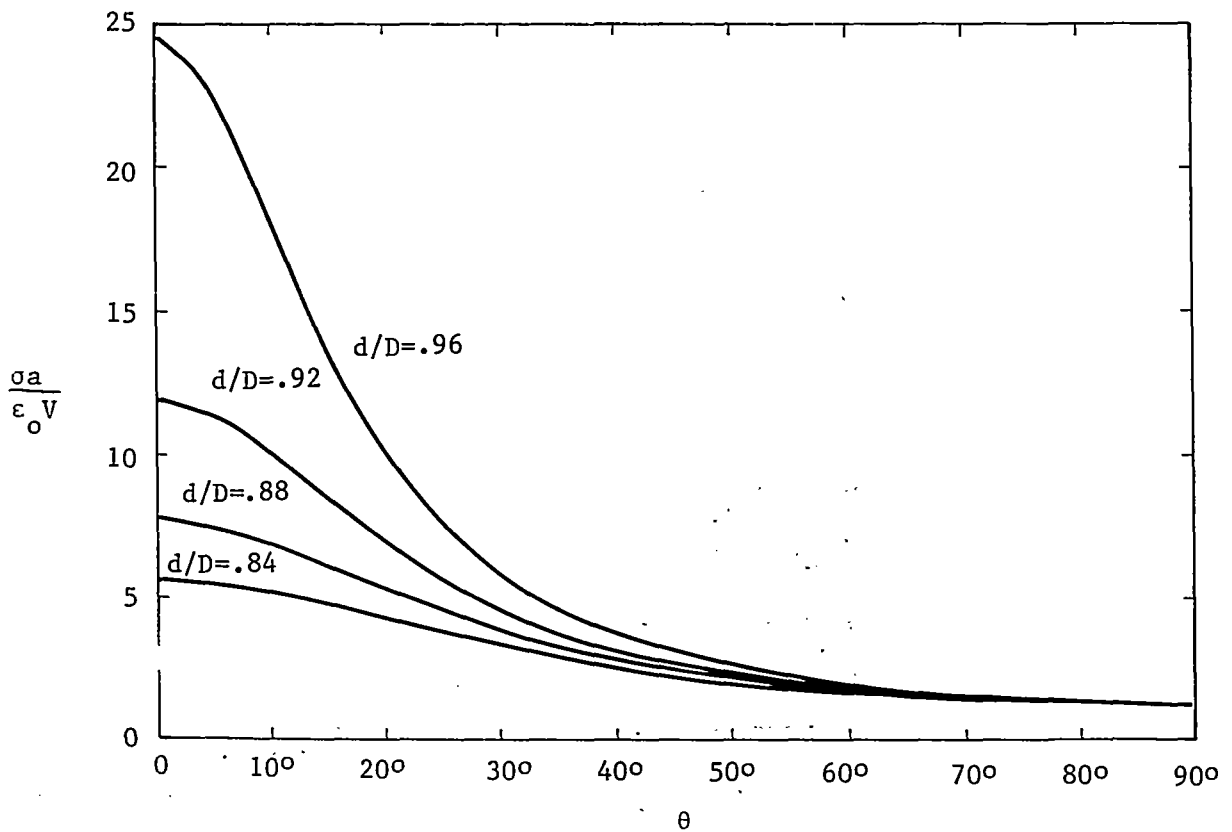


FIGURE 5B: CHARGE DENSITY ON LARGE CYLINDERS, LINE DRIVEN BETWEEN CYLINDER AND PLATES

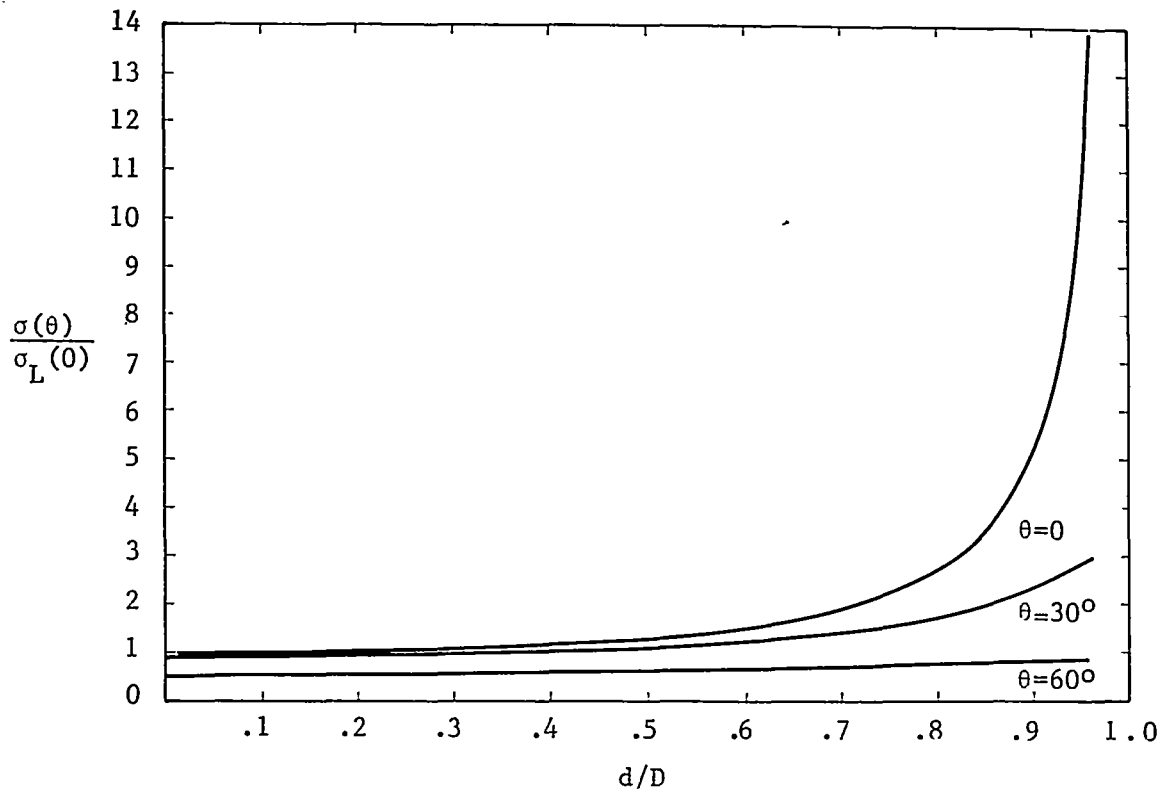


FIGURE 6A: CHARGE DENSITY AT POINTS ON THE CYLINDER AS A FUNCTION OF CYLINDER SIZE (CASE 1)

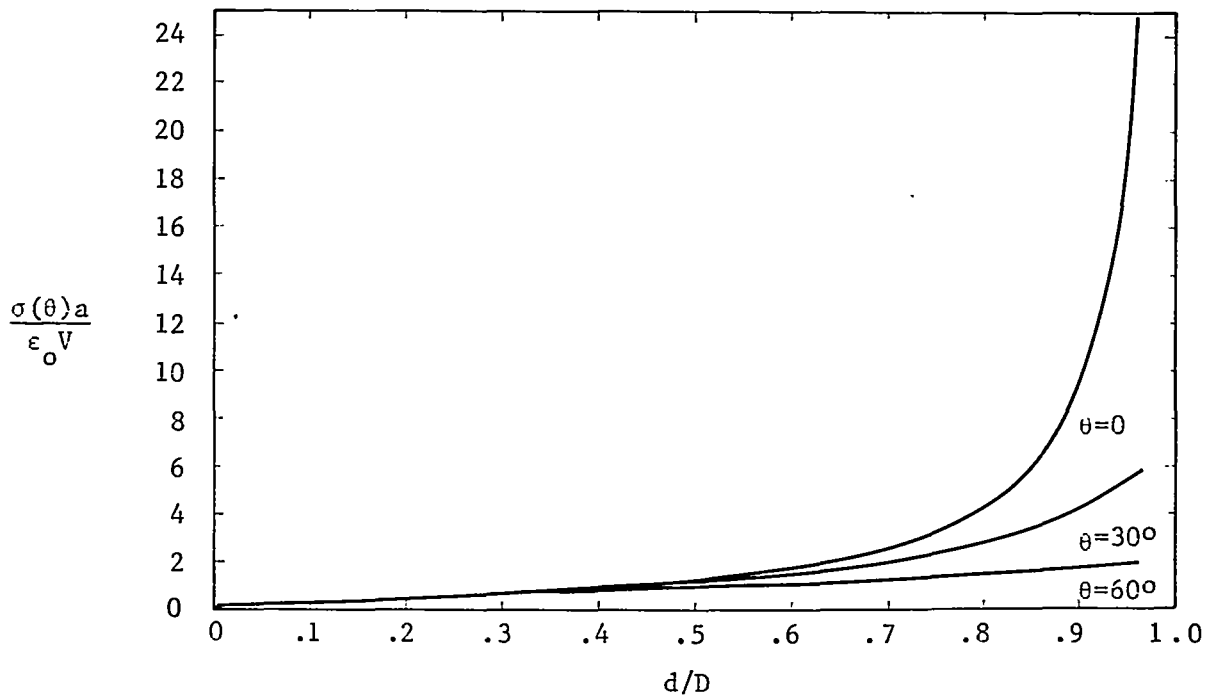


FIGURE 6B: CHARGE DENSITY AT POINTS ON THE CYLINDER AS A FUNCTION OF CYLINDER SIZE (CASE 2)

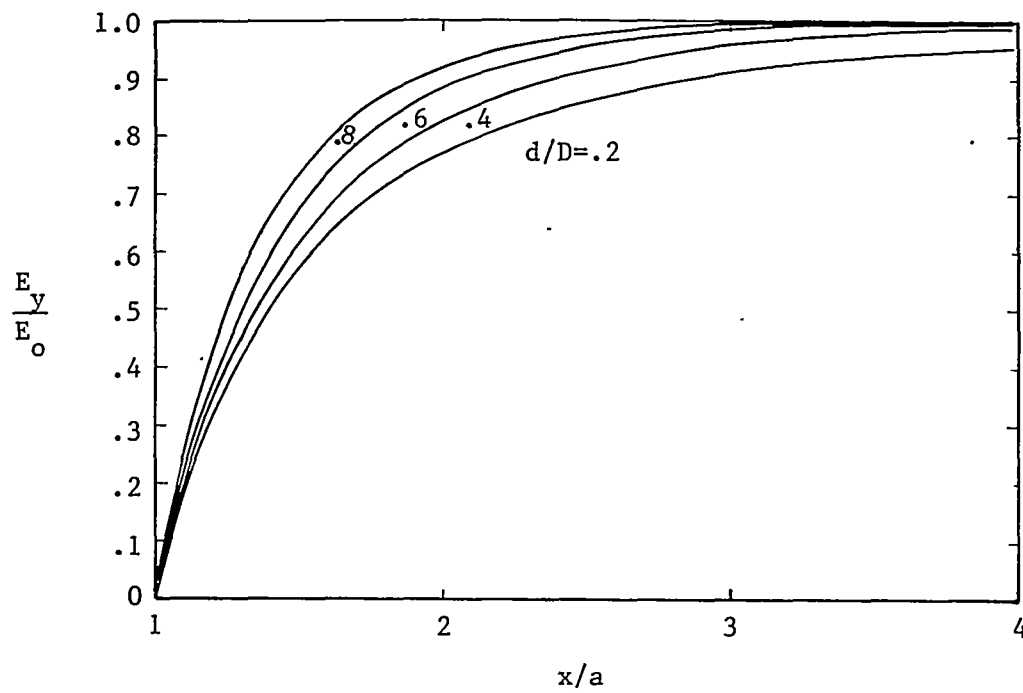


FIGURE 7A: ELECTRIC FIELD AT MID-POINTS
FOR SMALL CYLINDERS

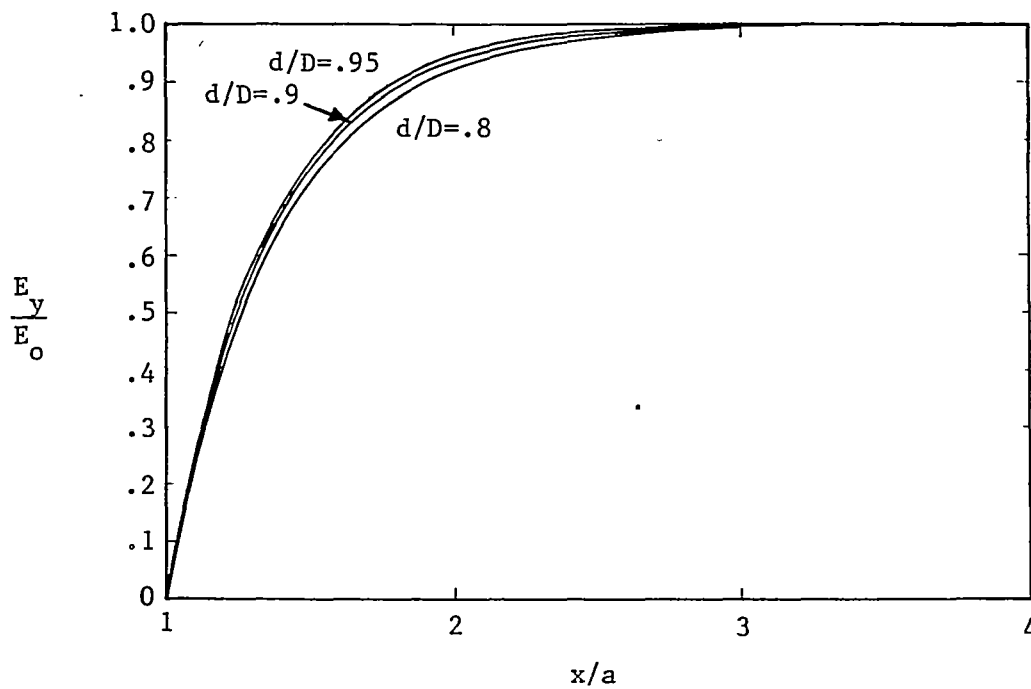


FIGURE 7B: ELECTRIC FIELD AT MID-POINTS
FOR LARGE CYLINDERS

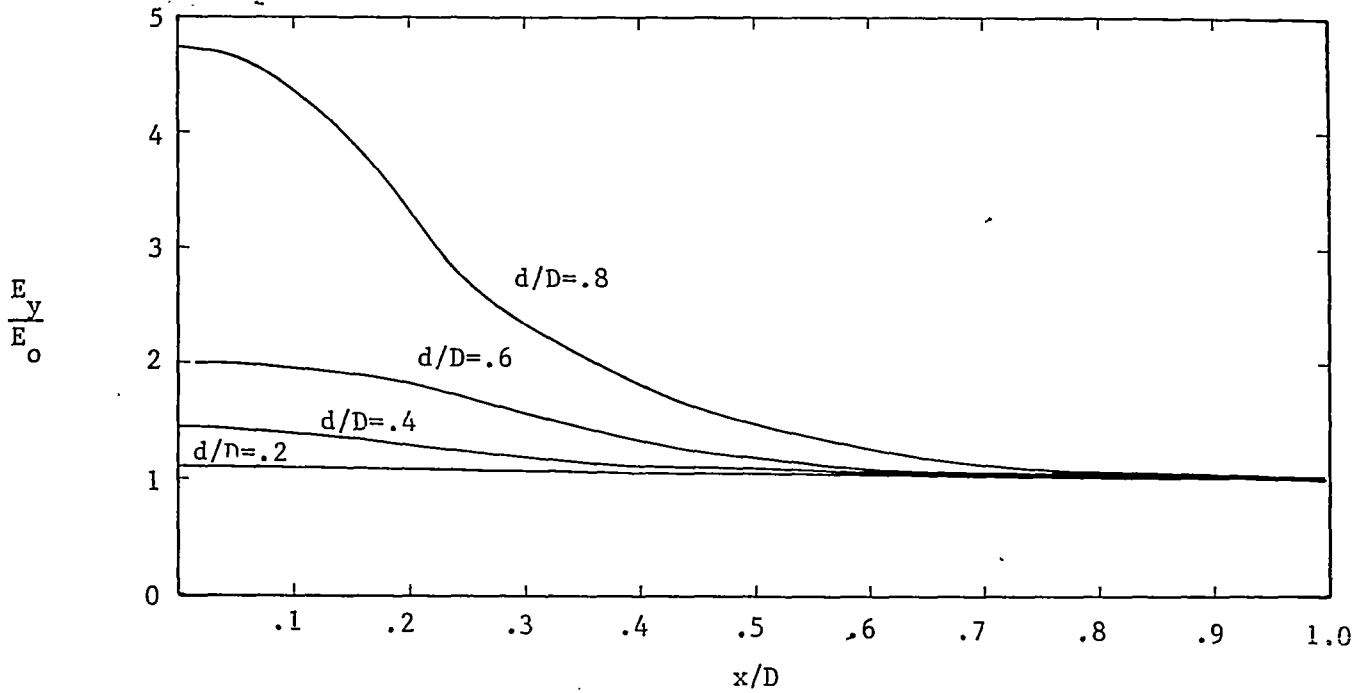


FIGURE 8A: ELECTRIC FIELD AT TOP PLATE FOR SMALL CYLINDERS

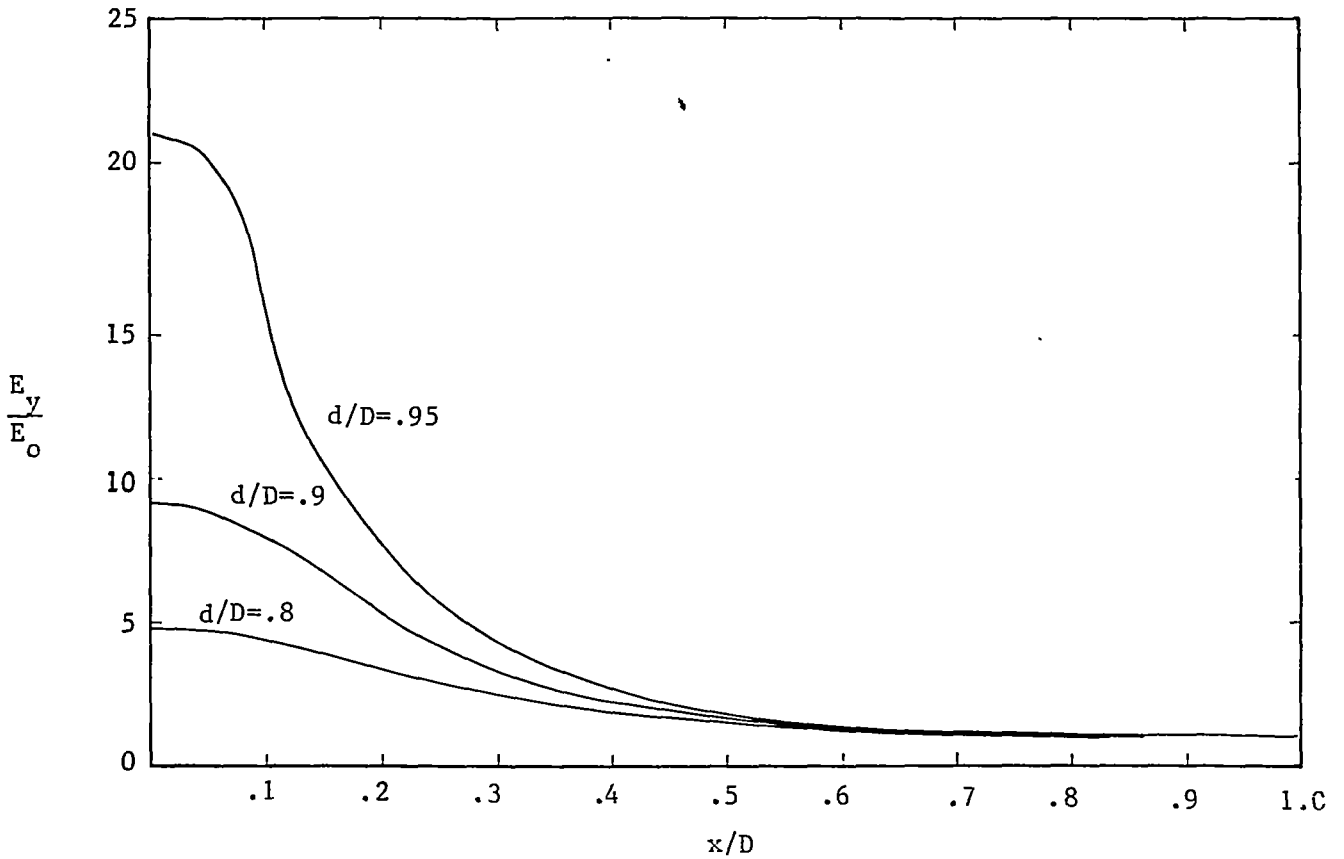


FIGURE 8B: ELECTRIC FIELD AT TOP PLATE FOR LARGE CYLINDERS

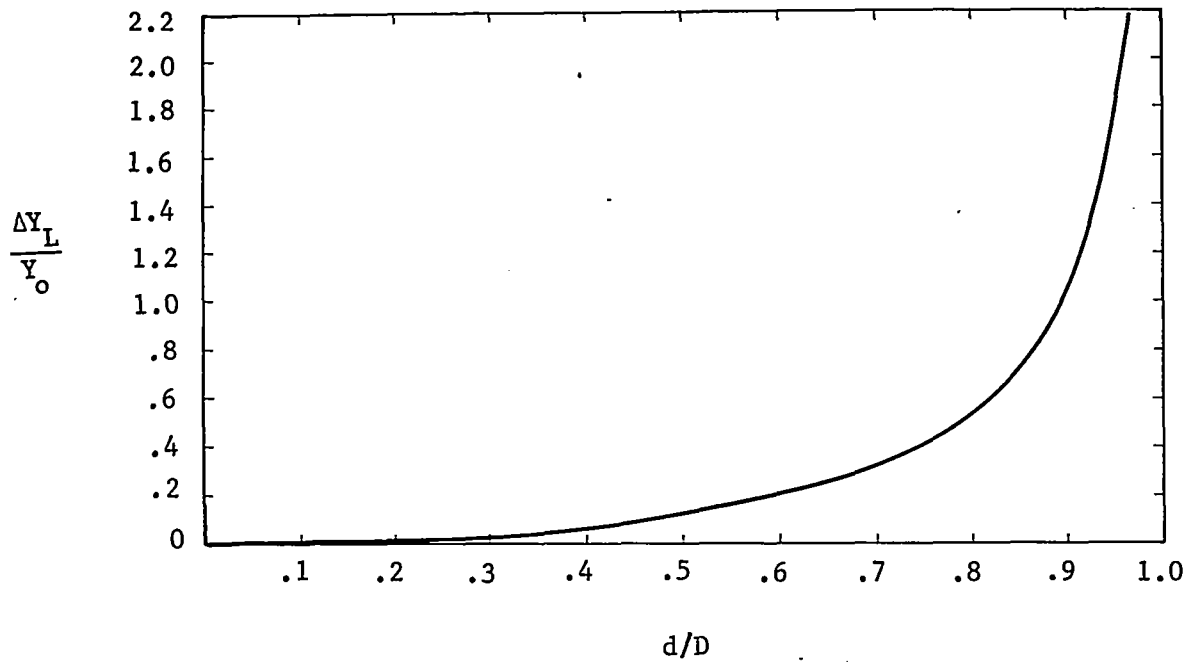


FIGURE 9A: INCREMENTAL ADMITTANCE DUE TO A CYLINDER IN A PARALLEL PLATE LINE

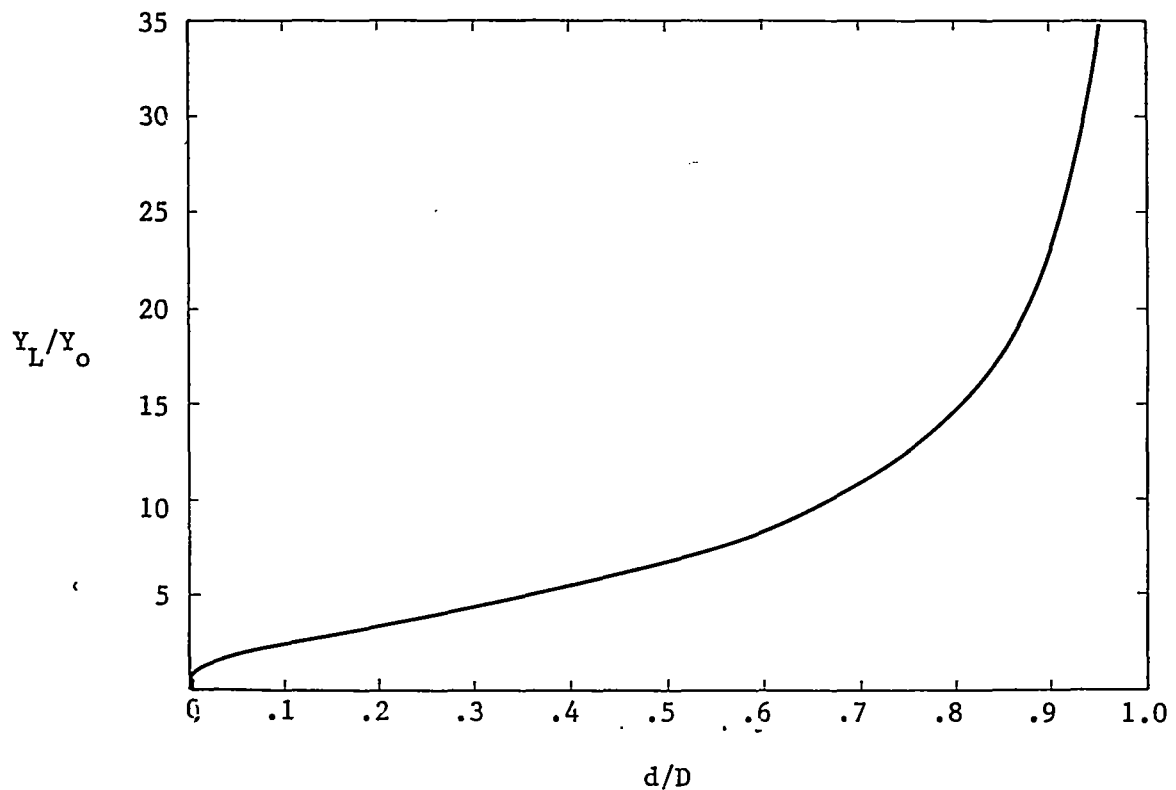


FIGURE 9B: INPUT ADMITTANCE OF THE LINE DRIVEN BETWEEN THE CYLINDER AND THE PLATES

Appendix A

If a cylindrical distribution of surface charge depends on the angular variable θ_m shown in figure 2 as

$$\sigma_{n,m}(\theta_m) = s_{n,m} \cos n\theta_m \quad (A-1)$$

then the potential due to this charge is given, outside the cylinder, by

$$\phi_e = \frac{s_{n,m} a}{2n\epsilon_0} \left(\frac{a}{r_m}\right)^n \cos n\theta_m \quad (A-2)$$

while inside the cylinder it is given by

$$\phi_e = \frac{s_{n,m} a}{2n\epsilon_0} \left(\frac{r_m}{a}\right)^n \cos n\theta_m \quad (A-3)$$

Now if the constants s_n are assumed to be those describing the charge on the primary cylinder of figure 2 then equations (2) and (A-2) clearly indicate that the potential of the charge on the m^{th} cylinder of figure 2 is

$$\phi_e = \sum_{n=1}^{\infty} (-1)^{n+m} \frac{s_n a}{2n\epsilon_0} \left(\frac{a}{r_m}\right)^n \cos n\theta_m \quad (A-4)$$

as long as this m^{th} cylinder carries no net charge. Adding the potential of all the image cylinders according to equation (A-4) gives the double summation in equation (3) of Section II.

The effect of a net charge on the primary cylinder may be accounted for by a logarithmic conformal transformation of the analytic function describing the potential of a line above a plane. This process leads to the equation for the potential of the net charge in the form

$$\phi_e = \frac{s_o a}{\epsilon_o} \operatorname{Re} \ln \left(\frac{e^{\pi Z/D - i\pi y_o/D}}{e^{\pi Z/D + i\pi y_o/D}} \right) \quad (\text{A-5})$$

where

$$Z = x + i(y+D/2)$$

If one expands equation (A-5) the logarithmic term of equation (3) is obtained and so the derivation of (3) is complete.

A procedure similar to the above, replacing equation (A-2) by equation (A-3) where it is appropriate, may be used to obtain equation (4) of Section II.

Appendix B

It is to be shown that if

$$f(x) = \sum_{n=1}^{\infty} (-1)^n \ln \tanh \left(\frac{n\pi x}{2} \right) \quad (B-1)$$

then

$$f(x) = \frac{1}{2} \ln \frac{1}{x} + f\left(\frac{1}{x}\right) \quad (B-2)$$

Since equation (B-2) is obviously true if x is unity, it is only necessary to demonstrate the equality of the derivatives of the two members of (B-2). In other words it is necessary to show that if

$$F(x) = \sum_{n=1}^{\infty} (-1)^n n\pi \operatorname{csch} n\pi x \quad (B-3)$$

then

$$F(x) = -\frac{1}{2x} - \frac{1}{x^2} F\left(\frac{1}{x}\right) \quad (B-4)$$

But by the Poisson summation formula⁶ and a table of integral transforms⁷ it may be shown that

$$F(x) = -\frac{1}{2x} + \frac{\pi}{2x^2} \sum_{n=0}^{\infty} \operatorname{sech}^2 \left(\frac{\pi}{2x} (2n+1) \right) \quad (B-5)$$

while, by expanding each term in the series of (B-5) as an infinite sum of exponentials and then interchanging the order of summation, equation (B-5) takes

the form of equation (B-4). Q.E.D.

Equation (B-2) and (B-4) are only two of several similar relations that arise in the study of electrostatic problems involving two-dimensional lattices. Another relation of the same nature is that if

$$G(x) = x/6 - x \sum_{n=1}^{\infty} \operatorname{csch}^2(n\pi x) \quad (\text{B-6})$$

then

$$G(x) + G(1/x) = 1/\pi \quad (\text{B-7})$$

References

1. Carl E. Baum, Sensor and Simulation Note 22 , "A Transmission-Line EMP Simulation Technique for Buried Structures", June, 1966.
2. Lord Rayleigh, Phil. Mag. 34, 481, 1892.
3. Milton Abramowitz and Irene A. Stegun, Editors, Handbook of Mathematical Functions, National Bureau of Standards, AMS-55, June, 1964, p. 804.
4. Philip M. Morse and Herman Feshbach, Methods of Theoretical Physics, Vol. II, McGraw-Hill, 1953, p. 1210.
5. James Clerk Maxwell, A Treatise on Electricity and Magnetism, Vol. I, Dover edition, 1954, p. 224.
6. R. Courant and D. Hilbert, Methods of Mathematical Physics, Vol. I, Interscience, 1953, p. 76.
7. A. Erdelyi, Editor, Tables of Integral Transforms, Vol. I, McGraw-Hill, 1954, p. 120.

THIS PAGE INTENTIONALLY BLANK

UNCLASSIFIED

Security Classification

DOCUMENT CONTROL DATA - R & D

(Security classification of title, body of abstract and indexing annotation must be entered when the overall report is classified)

1. ORIGINATING ACTIVITY (Corporate author) General Electric Company, TEMPO 816 State Street Santa Barbara, California 93102		2a. REPORT SECURITY CLASSIFICATION UNCLASSIFIED	
		2b. GROUP	
3. REPORT TITLE ELECTROMAGNETIC PULSE SENSOR AND SIMULATION NOTES, VOLUME 3 NOTES 44 through 55			
4. DESCRIPTIVE NOTES (Type of report and inclusive dates)			
5. AUTHOR(S) (First name, middle initial, last name)			
6. REPORT DATE July 1971	7a. TOTAL NO. OF PAGES 462	7b. NO. OF REFS	
8a. CONTRACT OR GRANT NO. F29601-70-C-0010	9a. ORIGINATOR'S REPORT NUMBER(S) AFWL EMP 1-3		
b. PROJECT NO.	9b. OTHER REPORT NO(S) (Any other numbers that may be assigned this report)		
c.			
d.			
10. DISTRIBUTION STATEMENT This document is subject to special export controls and each transmittal to foreign governments or foreign nationals may be made only with prior approval of AFWL (WLRE), Kirtland AFB, New Mexico, 87117. Distribution is limited because of the technology discussed in the reports.			
11. SUPPLEMENTARY NOTES		12. SPONSORING MILITARY ACTIVITY Air Force Weapons Laboratory (WLRE) Kirtland Air Force Base New Mexico 87117	
13. ABSTRACT A series of 12 notes on electromagnetic pulse sensor and simulation techniques. Subjects covered in this volume are: The Capacitor Driven, Open Circuit, Buried Transmission-Line Simulator; Electromagnetic Scattering from a Conducting Post; The Single-Conductor, Planar, Uniform Surface Transmission line, Driven from One End; The Diffraction of an Electromagnetic Plane Wave at a Bend in a Perfectly Conducting Planar Sheet; The Planar, Uniform Surface Transmission Line Driven from a Sheet Source; The Buried-Transmission-Line Simulator Driven by Multiple Capacitive Sources; The Buried-Transmission-Line Simulator with an Inductive Energy Source; Minimization of Induced Currents by Impedance Loading; A Parameter Study of Two Parallel Plate Transmission-Line Simulators of EMP Sensor and Simulation Note 21; Admittance Sheets for Terminating High-Frequency Transmission Lines; Matching the Impedance of Multiple Transitions to a Parallel-Plate Transmission Line; Interaction Between a Cylindrical Test Body and a Parallel Plate Simulator. Additional notes in this series will be published in subsequent volumes.			

DD FORM 1473
1 NOV 66REPLACES DD FORM 1473, 1 JAN 64, WHICH IS
OBSOLETE FOR ARMY USE.

UNCLASSIFIED

*U.S. GOVERNMENT PRINT OFFICE: 1971 - 432-810/3012

Security Classification